Journal of Physics: Conference Series **688** (2016) 012080 doi:10.1088/1742-6596/688/1/012080

Modern trends in low-density materials for fusion

A.S. Orekhov[1], A.A. Akunets[1], L.A. Borisenko[1,2], A.I. Gromov[1], Yu.A. Merkuliev[1], V.G. Pimenov[3], E.E. Sheveleva[3], V.G. Vasiliev[4], N.G. Borisenko[1,5]

[1] P.N. Lebedev Physical Institute of RAS, Russia
[2] Lomonosov Moscow State University, Russia
[3] N.D. Zelinsky Institute of Organic Chemistry RAS, Russia
[4] A.N. Nesmeyanov Institute of Organoelement Compounds of RAS, Russia
[5] National Research Nuclear University MEPhI (Moscow Engineering Physics Institute)

E-mail: orekhov@sci.lebedev.ru

Abstract. Low-density targets continue to yield new experimental data and to put new unsolved questions for driver-plasma experiments. The experiments with such targets are presented in the paper by "Low-density targets that worked in direct and indirect experiments with laser and particle beams" by L.A. Borisenko *et. al.* ibid.
Here we concentrate on nanostructured and aerogel targets' fabrication and characterization. These configurations establish certain standards for contemporary shot experiments.

1. Introduction

A variety of techniques is developed and used in order to meet the demand of laser interaction experiments with low-density targets. Different methods are worked out for typical requests below.

Extra fine regular structure is normally ordered to eliminate chaotic instability growth. Definite material structuring is used for plasma instability control or saturation through small-scale structures.

Mass gradients in targets are planned for different designs. Sharp density gradient is required for shock pressure multiplication. Z-gradient could be applied for preheating or energy-release control.

Thin aerogel or nano-snow layers are proved to smooth laser light before target illumination. Thin low-density metal layer on the inside of indirect target raises efficiency of hohlraum.

Well measured parameters and profoundly characterized structures of the target are obligatory for modern laser experiment success. This responsibility is a challenge because the hierarchies of needed parameters vary from experiment to experiment and from facility to facility. Most frequently the fabrication and metrology become unique and inventive.

2. Low-density polymer

Structured targets of definite and accurately measured features are requested for laser-plasma experiments and ICF applications, sometimes independently of the solid-matter physics capabilities. The targets' materials have become thin and light-weighted, so numerous problems occur during their characterization. This brings us to development of following instruments:

- better "traditional" diagnostic tools;
- customized software for existing devices;

- specific applications of common equipment;
- verification in the laser experiments in order to simplify the theoretical requirements on target.

Current fabrication process allows some control of the structures in a wide density range. Examples of structures, fabricated independently and in different time are given in Figure 1. The density is known from chemical solution composition.

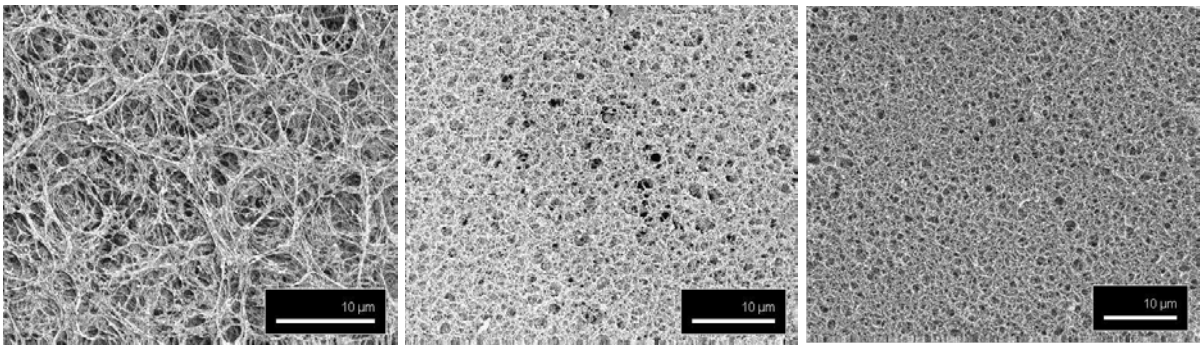

Figure 1. Structure of cellulose triacetate (CTA) aerogel with density 2 mg/cc (left), 5 mg/cc (centre), and 10 mg/cc (right). Scale is 10 µm; solid density is about 1.1 g/cc.

The methods of light materials characterization often result in sample destruction. So we search for stable techniques to produce repeatable fusion targets.

The experiments on high-temperature and high-pressure physics, shock front and implosion studies consume targets with density gradient. Approximately the gradient can be achieved by composing several layers with different densities. For higher efficiency smooth density gradient is needed.

Pressure multiplication in plasma with density increase [1] started our development of the shell target with smooth density gradient 30 mg/cc up to 20 g/cc in a single shell instead of double shell. Several methods are known for one-step production of density gradient samples. Those were performed and reported earlier by N.G. Borisenko *et al*. and W. Nazarov *et al.* [2]. Density profile monitoring during polymerization process indicates certain restrictions. Sharp density gradient (more than 1000 mg/cc/mm) is hard to produce. The supercritically dried divinyl benzene (DVB) aerogel with density gradient up to 400 mg/cc/mm done in University of St. Andrews (UK) was characterized with X-ray tomography (Figure 2).

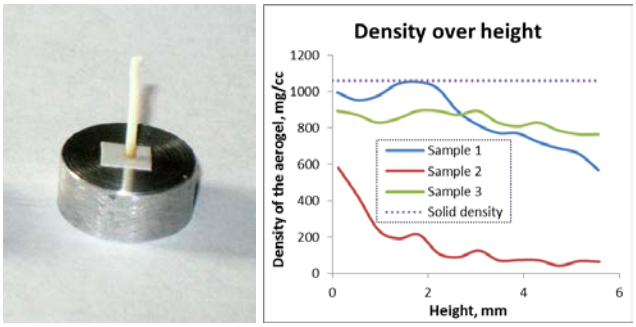

Figure 2. DVB aerogel fixed on tomograph metal mounting (left); dried DVB aerogel density via height for several different examined samples (right).

Sample 1 reaches full solid density at denser part, which looks optically transparent there. The rest two samples are opaque with visible gradual change of turbidity. But x-rays show only one of them (sample 2) displays density gradient, whereas sample 3 has altered structure rather than density over height. The optimization of manufacturing conditions should be worked out. Now we can only use x-rays based selection for needed gradient search.

The autowaves appear in the existing technology route of aerogels with smooth density gradient, reciprocal diffusion of catalyst and monomer are to be analyzed. Opposing diffusion of monomer and catalyst during polymer (samples of polystyrene) or silica gel synthesis/casting causes density modulations in the resulting vertical density gradient. The density waves during synthesizing polymer appear in case of decreasing monomer concentration which stimulates opposing diffusion of monomer and catalyst. The reaction is exothermic, and temperature contributes to acceleration of the reaction

rate. During silica gel polymerization the tetraethoxysilane solution produces not only heat but water which intensifies gelation. The acceleration causes sharp decrease over height of monomer concentration and results in lower density in the region with low monomer amount. This process finishes only on the top boundary of the monomer solution.

Different chemical systems have demonstrated modulation in density gradient, so quantitative study of autowaves in gradient gel growth is due to find regimes to eliminate or to damp them.

3. Low-density metal

We produce metal nano-snow layers of Bi or Au with 50-300 mg/cc density, pore sizes ~20 μm and solid elements (chains of metal nanoparticles) of ~100 nm diameter.

Subsequent thermal treatment and pressing result in layers density 0.2-4 g/cc, pores being twice or 2.5 times less than predicted, and average particle size increase up to 150-200 nm.

Metal nanoparticles and foam layers are produced inside a special setup according to a widely used technique of metal fog precipitation in the low-pressure buffer gas atmosphere (pure N, Ar or He). Heater evaporates solid metal forming dense atomic metal flow. At 1-5 Torr pressure in the setup chamber (1.5 meter high) metal fog or snow from nanoparticles is formed. Nanoparticle final size depends on pressure and buffer gas composition. Thus using of He results in tinier particles and lower densities, than Ar. The optimum pressure for target densities less than 1/100 of solids is known to be 150-700 Torr. Varying the conditions for fog production (heater temperature, gas composition, and pressure) and precipitation conditions (holder temperature) we can form nanoparticle layers down to 1-0.4% of solid metal density.

Hot melt is evaporated in 3-20 minutes, whereas precipitation lasts for 16-48 hours. Layer inner structures (Figure 3) may be globular, or may form fractal layers. The structure is self-similar in different scales (10-20 μm and 200-400 μm). SEM picture shows pores of 1-10 μm size.

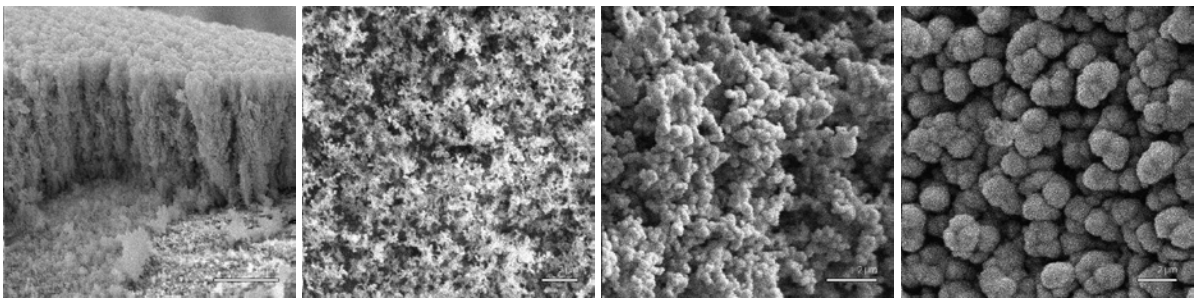

Figure 3. Left to right: cut of Bi snow layer, scale 20 μm; Sn snow layer, scale 2 μm; Cu snow layer, scale 2 μm; Bi snow layer, globules, scale 2 μm.

Parameters of thin low-density metal layer on the holders were examined using a carbon cylinder ("witness" of manufacturing) [3]. The witnesses are situated upright near the working samples during precipitation process, so they have the same low-density metal layer as on the final samples.

Due to symmetric horizontal shape of the witness we know the optical path and measure optical density of the sample on one X-rays photo. With absorption ratio restored from solid calibration wedge we can calculate the density of the sample. The thickness of the target layer is calculated as height of the "cup" on top the witness. We use simple formulas to recover thickness:

$$t = \frac{\rho}{\rho_{solid}} \cdot x,$$

where x is an absorption thickness in μm, ρ is the density of the layer, ρ_{solid} is the density of pure material. Then

$$I = I_0 \cdot e^{-\mu \cdot t},$$

where I and I_0 is the x-ray intensity after and before the sample, μ is absorption ratio in μm^{-1}.

Resulting thickness of analysed samples was about 40-150 μm with density varying from 40 to 180 mg/cc for bismuth layers and from 80 to 200 mg/cc for gold ones.

4. Low-density polymer and metal composites

Several types of high-Z nanoparticle dopants with different properties may help to explore increasing uniform compression. Steps in density profile ranging from subcritical (about 2 mg/cc) to 100 mg/cc are reported for higher hydrodynamic efficiency of targets. Layers with density gradient are required for equation-of-state (EOS) experiments. Concentration profile of high-Z nanoparticles in aerogel layers is planned for increasing of target efficiency, and for efficient x-ray converters.

Metal densities of less than 100 mg/cc (to as low as 10 mg/cc) are obtained in composites of heavy metal nanoparticles (50-100 nm diameter) inside the polymer network with solid fibers of 0.1 μm size and 3 μm apart. The polymer can contain up to 20% by weight (wt) for Cu nanoparticles and up to 50% (wt.) for Au nanoparticles. Earlier we saw coarser structure of Cu-loaded aerogel [4].

Now the structure of CTA aerogel remains the same (Figure 4) when metal nanoparticle doping is moderate (<30%). In this case inert (plastic) mass and non-uniformities are minimized, when nanoparticles are kept inside the interaction volume for cluster-related laser experiments.

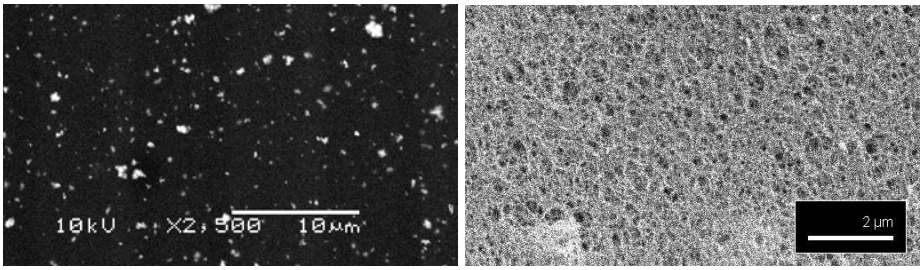

Figure 4. X-ray analysis by self-emission of Cu nanoparticles in CTA film, scale 10 μm (left); structure of 10 mg/cc CTA aerogel with 20% (wt) of Cu nanoparticles, scale 2 μm (right).

5. Conclusions

The following distinct trends seem to prevail in low-density target manufacturing techniques.

1. Nanostructuring and uniformity are combined with a wide range of densities requested, from 1-2 mg/cc (gas-like) to more than 100 mg/cc. Polymer foams give way to plastic aerogels – fine uniform materials for easy simulations and comparison with experimental results. Plastic aerogels with quasiperiodic tiny structure are now available for manufacturing within certain range of parameters. Different experimental techniques are used for manufacturing of extremely low and of moderate densities.
2. Metal nano-snow layers are sometimes sintered for better stability. Low-density metals are useful in many respects. Their regularity is reached close to that of plastic aerogels.
3. Combinations and topologic modifications are possible. Composites, metal nanoparticles in plastic matrix are the examples. In fact the diversity of structures now used in laser experiments came to some desired standards, where aerogels and nanostructures remain the preferred form.

References

[1] D. Batani et al., Phys. Rev. E, 2001, V. 63, 046410

[2] N.G. Borisenko, A.A. Akunets, et al. Fusion science and technology, 2009, V. 55, №4, pp. 477-483.
N. G. Borisenko, W. Nazarov, et al., Journal of Radioanalytical and Nuclear Chemistry, 2014, V. 299, №2, pp. 961-964; DOI 10.1007/s10967-013-2628-2

[3] L.A. Borisenko, A.S. Orekhov, et al., Journal of Radioanalytical and Nuclear Chemistry, 2014, V. 299, №2, pp.955-960; DOI 10.1007/s10967-013-2629-1
I.V. Akimova, N.G. Borisenko, et al., Problems of Atomic Science and Technology, ser. Thermonuclear Fusion, 2012, №2, pp. 122-130 (in Russian).

[4] N.G. Borisenko, et al., Fusion Sciences and Technology, 2006, V. 49, №4, pp. 676-685.